

## Formation and evolution of bulges

E. Athanassoula<sup>1</sup> and I. Martinez-Valpuesta<sup>1,2</sup>

<sup>1</sup>*LAM, OAMP, 2 place Le Verrier, 13248 Marseille cedex 04, France*

<sup>2</sup>*IAC, E-38200 La Laguna, Tenerife, Spain*

**Abstract.** After presenting three ways of defining a bulge component in disc galaxies, we introduce the various types of bulges, namely the classical bulges, the boxy/peanut bulges and the disc-like bulges. We then discuss three specific topics linked to bulge formation and evolution, namely the coupled time evolution of the bar, buckling and peanut strengths; the effect of velocity anisotropy on peanut formation; and bulge formation via bar destruction.

### 1. What is a bulge?

Three ways of defining a bulge have been used so far, one morphological, the second photometrical and the third kinematical. Based on morphology, a bulge is a component of a disc galaxy that has a smooth light distribution that swells out of the central part of a disc viewed edge-on. This definition has the disadvantage of being applicable only to edge-on systems and the advantage of necessitating only an image of the galaxy. The second definition is based on photometry and defines a bulge as the extra light in the central part of the galaxy, above the exponential profile fitting the remaining (non central) part of the disc. In earlier papers this component was fitted with an  $r^{1/4}$  law, while more recent ones use its generalisation to an  $r^{1/n}$  law (Sérsic 1968). This definition has the advantage of being applicable to disc galaxies independent of their inclination. It has also the advantage of leading to quantitative results about the light distribution, but has the disadvantage of assigning to the bulge any extra central luminosity of the disc, independent of its origin. The third definition is based on kinematics, and in particular on the value of  $V/\sigma$ , or more specifically on the location of the object on the ( $V/\sigma$ , ellipticity) plot, which is often referred to as the Binney diagram (Binney 1978, 2005). This definition, potentially quite powerful, has unfortunately been very little used so far, due to the small number of galaxies for which the necessary data are available, a situation which is rapidly improving with large surveys, such as SAURON (Bacon *et al.* 2001; de Zeeuw *et al.* 2002; Peletier this volume).

The lack of a single, clear-cut definition of a bulge is due to the fact that disc galaxies are viewed in different orientations and also to the fact that not all types of data are available for all objects. Nevertheless, it has led to considerable confusion and to the fact that bulges are an inhomogeneous class of objects. Indeed, many different types of objects, with very different properties and formation histories are included in the general term ‘bulges’. To remedy this, Kormendy (1993) and Kormendy & Kennicutt (2004) distinguish classi-

cal bulges from pseudo-bulges, the latter category encompassing all bulges that are not classical. Athanassoula (2005a) argues that pseudo-bulges also are an inhomogeneous class of objects, and thus distinguishes three types of bulges.

**Classical bulges** are formed by gravitational collapse or hierarchical merging of smaller objects and corresponding dissipative gas processes. The material forming this bulge could be externally accreted, or could come from clumps in the proto-disc. In general, bulges of this type are formed before the actual disc (e.g. Steinmetz & Müller 1995; Noguchi 1998; Immeli *et al.* 2004). Nevertheless, a bulge can also form from material externally accreted at much later stages (e.g. Pfenniger 1991; Athanassoula 1999; Aguerri, Balcells & Peletier 2001; Fu, Huang, Deng 2003). Their morphological, photometrical and kinematical properties are similar to those of ellipticals.

**Box/peanut bulges** (B/P) form from a vertical instability of the disc material. This has often been observed in  $N$ -body simulations of bar-unstable discs, where the initial stage of bar formation is followed by a puffing up of the inner parts of the bar (e.g. Combes & Sanders 1981; Combes *et al.* 1990; Raha *et al.* 1991; Athanassoula & Misiriotis 2002; Athanassoula 2003, 2005a; O’Neil & Dubinski 2003; Martinez-Valpuesta & Shlosman 2004; Debattista *et al.* 2004, 2006; Martinez-Valpuesta *et al.* 2006). Viewed side-on (i.e. edge-on with the line of sight along the bar minor axis), this structure protrudes from the disc and has a characteristic boxy or peanut shape whose size is of the order of a few disc scale-lengths. Thus, a box/peanut bulge is just *part* of a bar seen side-on.

Finally **disc-like bulges** form from inflow of (mainly) gas material to the centre of the galaxy and subsequent star formation (e.g. Athanassoula 1992; Friedli & Benz 1993; Heller & Shlosman 1994; Wada & Habe 1995). The torque exerted by the bar pushes gas, and to a lesser extent also stars, to the inner parts of the disc where they form an inner disc. Star formation can be very high there, due to the increased gas density. Thus the result of this process should be a central disc, or disc-like object, whose stellar component should include a sizable fraction of young stars and whose size should be less than, or of the order of a kpc. Such a component could harbour sub-structures such as spirals, or bars, as is indeed sometimes observed (Kormendy & Kennicutt 2004 and references therein). It is thus clear that disc-like bulges are very different objects from boxy/peanut bulges, since they are much smaller, have a different shape, different kinematics and provide a different type of excess on the radial photometric profiles. They also have different formation histories.

The different formation histories of these three types of objects lead to different properties – morphological, photometrical and kinematical – which in turn help classify observed bulges into one of the three above mentioned types. Nevertheless, as stressed by Athanassoula (2005a), different types of bulges often co-exist and it is possible to find all three types of bulges in the same simulation, or galaxy.

Realising the non-homogeneity of the objects classified as bulges and attempting to classify them is only the first step. Much more work is now necessary, particularly on two issues. The first one is the understanding of the formation and evolution of these types of objects. The second one is to predict the properties of these objects, starting from their formation scenarios. The latter is particularly important in order to bridge the gap between classification

schemes based on formation histories and classification schemes based on observed properties. Here we make small contributions to both these issues, using  $N$ -body simulations. In Sect. 2 we present the time evolution of the bar, the buckling and the peanut strengths and their interplay. Sect. 3 discusses the velocity anisotropy and its link to the above strengths. Finally, in Sect. 4 we discuss the photometrical properties of a destroyed bar and boxy/peanut bulge.

## 2. Time evolution of the bar, buckling and peanut strengths

Formation of boxy/peanut bulges has been witnessed in a large number of simulations, starting with Combes & Sanders (1981). It is now well understood in terms of orbital structure and particularly in terms of the instability of the periodic orbits that constitute the backbone of the bar (Pfenniger 1984; Skokos, Patsis & Athanassoula 2002; Patsis, Skokos & Athanassoula 2002).

Time evolution of the bar, the buckling and the peanut strengths are plotted in Fig. 1 for a simulation which develops a strong bar. The time is given in computer units and, for a reasonable calibration, 100 computer units correspond to 1.4 Gyrs (Athanassoula & Misiriotis 2002). The initially unbarred disc forms a bar roughly between times 150 and 250 (lower panel). We define as bar formation time the time at which the bar-growth is maximum (i.e. when the slope of the bar strength as a function of time curve is maximum) and indicate it by the first vertical line in Fig. 1. The bar strength reaches a maximum at a time noted by the second vertical line, and then drops, at a time which is denoted by the third vertical line. It reaches a minimum, at a time given by the fourth vertical line and then starts increasing again. The upper panel shows the buckling strength, i.e. the vertical asymmetry as a function of time. Before the bar forms, the disc is vertically symmetric, with the first indications of asymmetry occurring after bar formation. Then the asymmetry grows very abruptly to a strong, clear peak and then drops equally abruptly. The time of the buckling is given by the peak of this curve and is very clearly defined. It is important to note that, to within the measuring errors, it coincides with the time of bar decay (third vertical line). This is not accidental. We verified this in a very large number of simulations and thus can establish the link between the buckling episode and the decay of the bar strength (Raha *et al.* 1991; Martinez-Valpuesta & Shlosman 2004). The middle panel shows the strength of the peanut as a function of time. This quantity grows abruptly with time after the bar has reached its maximum amplitude and during the time of the buckling. This abrupt growth is followed by a much slower increase over a long period of time. Taken together, these figures show that the bar forms vertically thin, and only after it has reached a maximum strength does the buckling phase occur. The time intervals during which bar formation, or peanut formation, or buckling occur are all three rather short, of the order of a Gyr or less, and they are followed by much longer times of slower bar and B/P evolution.

This particular simulation has a second, much weaker buckling episode around time 700. This occurs very often in simulations developing strong bars. It is seen clearly in the peanut strength development, as a second abrupt increase of the peanut strength (Athanassoula 2005b; Martinez-Valpuesta *et al.* 2006). There are indications for it in the buckling strength, but not in the bar

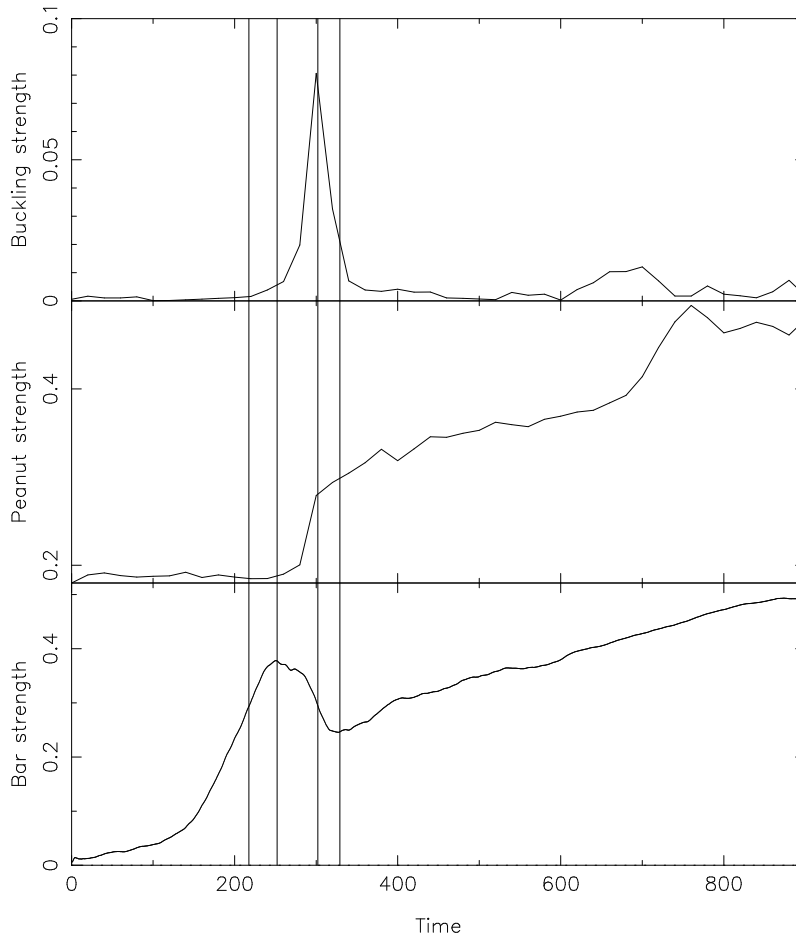


Figure 1. Time evolution of three peanut-, or bar-related quantities, namely the buckling strength (asymmetry; upper panel), the peanut strength (middle panel) and bar strength (lower panel). The thin vertical lines mark characteristic times linked to bar formation and evolution. From left to right, these are the bar formation time, the maximum amplitude time, the bar decay time and the bar minimum amplitude time (see text).

strength. As already mentioned, there are several possible definitions of the bar and the buckling strengths (Athanasoula & Martinez-Valpuesta, in preparation; Martinez-Valpuesta & Athanasoula, these proceedings) and exactly how clearly the buckling episodes are seen in time evolution plots depends somewhat on the definition adopted. For example, since the first buckling concerns more inner than outer parts (Martinez-Valpuesta *et al.* 2006), one can calculate the quantities in Fig. 1 using, instead of the whole disc, only the radial range mainly concerned by the first or by the second buckling, which allows to see better the buckling in question and its effects.

### 3. Velocity anisotropy and peanut formation

As already mentioned, peanut formation is linked to the vertical instability of parts of the main family of periodic orbits constituting the bar. This family is widely known as the  $x_1$  family. Its stability can be followed from the stability diagram (see e.g. figures 3 and 4 of Skokos *et al.* 2002) which show that, at the positions where  $x_1$  becomes unstable, other families bifurcate. These are linked to the  $n : 1$  vertical resonances and extend well outside the disc equatorial plane. As shown by Patsis *et al.* (2002), some of them are very good building blocks for the formation of peanuts, because they are stable and because their orbits have the right shape and extent. Thus, orbital structure theory can go a long way towards explaining the formation and properties of the peanut.

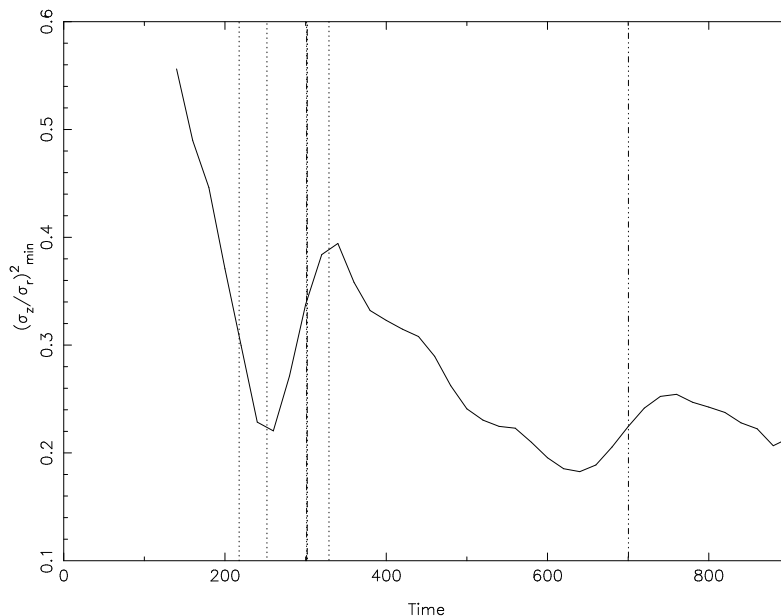


Figure 2. Time evolution of the ratio  $\sigma_z^2/\sigma_r^2$ . The thin vertical lines mark characteristic times linked to bar formation and evolution. From left to right, the first four ones are the bar formation time, the maximum amplitude time, the bar decay time and the bar minimum amplitude time, all corresponding to the first buckling episode (see text and Fig. 1). The fifth and last vertical line (dash-dot-dot-dot) marks the time of the second buckling.

An alternative approach explains the buckling and peanut formation as due to the bending, or fire-hose, instability, studied analytically in the linear regime (Toomre 1966; Araki 1985). These studies assign a critical value of  $R_\sigma = \sigma_z^2/\sigma_r^2$  igniting the onset of the instability, which is around 0.1. A number of simulations, however, have shown that this instability sets in already at much larger values (e.g. Merritt & Sellwood 1994; Sotnikova & Rodionov 2003).

To test this hypothesis, we calculate the radial and  $z$  components of the disc velocity dispersion as a function of radius (averaging over azimuth and height). We then find the minimum value of their ratio  $R_\sigma$  and plot its time evolution in Fig. 2. The thin vertical lines in this figure are at the locations

found from Fig. 1 and mark the characteristic times linked to bar formation and evolution; namely the bar formation time, the maximum amplitude time, the bar decay time and the bar minimum amplitude time. Their location is clearly linked to the various evolutionary phases of  $R_\sigma$ . This, however, need not necessarily be seen as the cause of the buckling, but can also be seen as its result. Indeed, as the bar forms  $\sigma_r$  increases drastically, so that  $R_\sigma$  decreases. Then, the bar amplitude reaches its maximum and starts decreasing, while the peanut starts forming. During this time,  $\sigma_r$  decreases, while  $\sigma_z$  increases. As a result, between these two time intervals the ratio  $R_\sigma$  should reach a minimum and then increase again, as is indeed seen in Fig. 2. Then the bar amplitude reaches a minimum, which corresponds to a minimum of  $\sigma_r$  and therefore to a maximum of  $R_\sigma$ . This is followed by a slow decrease of  $R_\sigma$ , which is stopped by the second buckling episode. The value of  $R_\sigma$  at which this instability sets in is much less extreme than that predicted by the above mentioned analytical works, but in good agreement with other  $N$ -body simulations.

More work is necessary before we fully understand the respective roles of the orbital structure results and of the velocity anisotropy effects on the formation and evolution of B/P structures. Both explain part of the story, but many aspects of their interplay are still unclear. Orbital structure results can tell us whether the appropriate building blocks are available, or not, and this is essential since the lack of the appropriate building blocks can prohibit the formation of a given structure. Furthermore, studies of the properties of the building-block orbits are essential for understanding the properties of the B/P structures. On the other hand, it is necessary to group all these building blocks into one coherent unit and here collective effects are essential. They also can place limits on the formation of B/P structures, as well as give information on their properties. We will discuss the respective input from the two methods further elsewhere.

#### 4. Bar and peanut destruction

The effect of a central mass concentration (CMC) on bar evolution has been well studied with the help of purely stellar  $N$ -body simulations, placing lower limits on the mass and central concentration necessary for the bar to be destroyed. Comparison with observations, however, shows that these limits are much higher than the measured values (Shen & Sellwood 2004; Athanassoula, Lambert & Dehnen 2005 and references therein), thus casting doubts as to whether it is possible to destroy bars in this way. On the other hand, simulations with an SPH, or sticky particle representation of the gas come to a different conclusion (e.g. Friedli & Benz 1993; Berentzen *et al.* 1998; Bournaud & Combes 2002). Whether the difference between the two types of simulations could be due to the role of the gas in the angular momentum exchange is still debated (Bournaud, Combes & Semelin 2005; Athanassoula *et al.* 2005; Berentzen *et al.* 2007). We will not attempt to settle the issue here. We will just study the photometric properties after the bar is destroyed, without worrying about whether the necessary CMC is compatible with observations, or not, or what the role of the gaseous component is. Our aim here is to see whether these photometric properties are compatible with those of a bulge, and, if yes, of what type of bulge.

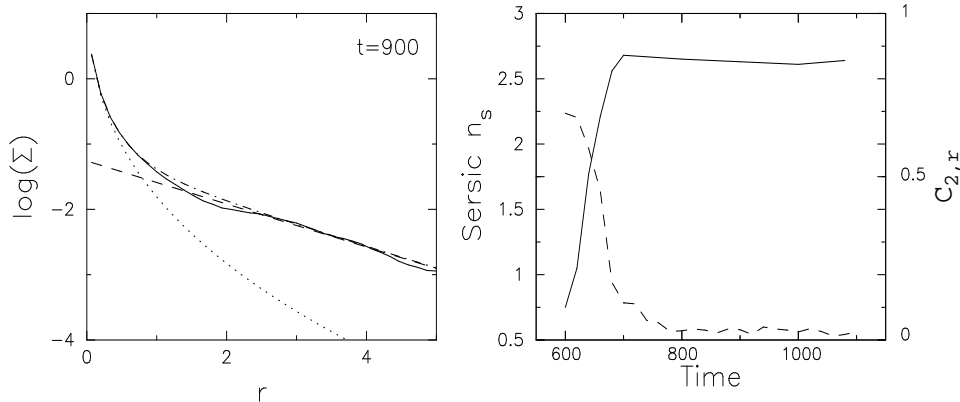


Figure 3. Bulge formation via bar destruction (see text). *Left panel* : Radial density profile of the luminous material (solid line) and its decomposition in a disc (dashed) and bulge (dotted) component. The sum of the two is given by a dash-dotted line. *Right panel* : Time evolution of the Sérsic index (solid line) and of the bar strength (dashed line). All quantities are in computer units as given by Athanassoula *et al.* (2005).

The simulations used in this analysis are those of Athanassoula *et al.* (2005). For several times in every simulation, we obtained the radial density profile, and then decomposed it into a disc and a bulge component, fitted by an exponential disc and a Sérsic profile, respectively. An example for a case with initially a strong bar with a clear peanut, in which we gradually grew a massive CMC, is shown in the left panel of Fig. 3. The corresponding value for the Sérsic index is  $n_s = 2.6$ , i.e. approaching the range of values found for classical bulges (e.g. Kormendy & Kennicutt 2004). We have performed this decomposition for several times during the simulation and plot the values of  $n_s$  as a function of time in the right panel of Fig. 3, where we also plot the bar strength as a function of time. For the simulation we are analysing, the CMC has been grown gradually in 100 computer units (600 - 700), or, equivalently, 1.4 Gyrs. We note that, during that time, the bar strength drops and  $n_s$  increases, both drastically, while after the CMC has reached its final mass, both values stay nearly constant. The final value of the Sérsic index depends on the mass of the CMC.

The above shows that, at least as far as the photometrical definition presented in Sect. 1 is concerned, a decayed bar can give rise to an object with a Sérsic profile approaching those of classical bulges. Its shape when the snapshot is viewed edge-on is compatible with that of a classical bulge. Thus, by two of the three definitions presented in Sect. 1, it is tempting to classify this object as a classical bulge. Work to study its kinematics is underway, in order to complete the classification and see whether such objects are compatible with classical bulges (Athanassoula, Aguerri & Martinez-Valpuesta, in preparation).

**Acknowledgments.** It is a pleasure to thank our collaborator, Alfonso Aguerri, for many interesting discussions and a fruitful collaboration, and A. Bosma, M. Balcells, P. Erwin, C. Heller, R. Peletier, M. Pohlen and I. Shlosman for stimulating discussions and encouragement. This work has been partially

supported by a Peter Grüber Foundation Fellowship to IMV and by grant ANR-06-BLAN-0172.

## References

- Aguerri, J. A. L., Balcells, M., Peletier, R. F. 2001, *A&A*, 367, 428  
 Araki, S. 1985 PhD thesis, MIT  
 Athanassoula, E. 1992, *MNRAS*, 259, 345  
 Athanassoula, E. 1999, in *Astrophysical Discs*, eds. J. A. Sellwood & J. Goodman, PASP conference series, 160, 351  
 Athanassoula, E. 2003, *MNRAS*, 341, 1179  
 Athanassoula, E. 2005a, *MNRAS*, 358, 1477  
 Athanassoula, E. 2005b, in *Planetary Nebulae as Astronomical Tools*, eds. R. Szczerba, G. Stasińska & S. K. Górný, AIP Conf. Proc. 804, Melville, New York, 333  
 Athanassoula, E., Misiriotis, A. 2002, *MNRAS*, 330, 35  
 Athanassoula, E., Lambert, J. C., Dehnen, W. 2005, *MNRAS*, 363, 496  
 Bacon, R. *et al.* 2001, *MNRAS*, 326, 23  
 Berentzen, I., Heller, C. H., Shlosman, I., Fricke, K. J. 1998, *MNRAS*, 300, 49  
 Berentzen, I., Shlosman, I., Martinez-Valpuesta, I., Heller, C.H. 2007, *ApJ*, in press  
 Binney, J. 1978, *MNRAS*, 183, 501  
 Binney, J. 2005, *MNRAS*, 363, 937  
 Bournaud, F., Combes, F. 2002, *A&A*, 392, 83  
 Bournaud, F., Combes, F., Semelin, B. 2005, *MNRAS*, 364L, 18  
 Combes, F., Sanders, R. H. 1981, *A&A*, 96, 164  
 Combes, F., Debbasch, F., Friedli, D., Pfenniger, D. 1990, *A&A*, 233, 82  
 Debattista, V. P., Carollo, M., Mayer, L., Moore, B. 2004, *ApJ*, 604, L93  
 Debattista, V. P., Carollo, M., Mayer, L., Moore, B., Wadsley, J., Quinn, T. 2006, *ApJ*, 645, 209  
 de Zeeuw, P. T. *et al.* 2002, *MNRAS*, 329, 513  
 Friedli, D., Benz, W. 1993, *A&A*, 268, 65  
 Fu, Y. N., Huang, J. H., Deng, Z. G. 2003, *MNRAS*, 339, 442  
 Heller, C. H., Shlosman, I. 1994, *ApJ*, 424, 84  
 Immeli, A., Samland, M., Gerhard, O., Westera, P. 2004, *A&A*, 413, 547  
 Kormendy, J. 1993, in *Galactic Bulges*, eds. H. Dejonghe and H. J. Habing, Kluwer Academic Publ., IAU Symposium 153, 209  
 Kormendy J., Kennicutt R. C. 2004, *ARA&A*, 42, 603  
 Martinez-Valpuesta, I., Shlosman, I. 2004, *ApJ*, 613, 29  
 Martinez-Valpuesta, I., Shlosman, I., Heller, C. 2006, *ApJ*, 637, 214  
 Merritt, D., Sellwood J. A. 1994, *ApJ*, 425, 551  
 Noguchi, M. 1998, *Nature*, 392, 253  
 O'Neill, J. K., Dubinski, J. 2003, *MNRAS*, 346, 251  
 Patsis, P., Skokos, Ch., Athanassoula, E. 2002, *MNRAS*, 337, 578  
 Pfenniger, D. 1984, *A&A*, 134, 373  
 Pfenniger, D. 1991, in *Dynamics of Disc Galaxies*, ed. B. Sundelius, Göteborg University Press, Göteborg  
 Raha, N., Sellwood, J. A., James, R. A., Kahn, F. D. 1991, *Nature*, 352, 411  
 Sérsic, J. 1968, *Atlas de Galaxias Australes*, Obs. Astron. Cordoba  
 Shen, J., Sellwood, J. A. 2004 *ApJ*, 604, 614  
 Skokos, H., Patsis, P., Athanassoula, E. 2002, *MNRAS*, 333, 847  
 Sotnikova, N. Ya., Rodionov, S. A. 2003, *AstL*, 29, 321  
 Steinmetz, M., Müller, E. 1995, *MNRAS*, 276, 549  
 Toomre, A. 1966, *Geophys. Fluid Dyn.*, N66-46, 111  
 Wada, K., Habe, A. 1995, *MNRAS*, 277, 433